

Chapter 2

Active Structural Control

Abstract This chapter provides an overview of building structure modeling and control. It focuses on different types of control devices, control strategies, and sensors used in structural control systems. It also discusses system identification techniques and some important implementation issues.

Keywords Structural control • Vibration attenuation • Mathematical modeling

2.1 Introduction

Structural vibration can be generally controlled in two ways: (1) by constructing the buildings using smart materials [2]; (2) by adding controlling devices like dampers, isolators, and actuators to the building [3–5]. In this work, we only discuss the latter case, where the structural dynamics are modified favorably by adding active devices. The performance of a structural control system depends on various factors including excitation type (e.g., earthquakes and winds), structural characteristics (e.g., degree of freedom, natural frequency, and structure nonlinearity), control system design (e.g., type and number of devices, placement of devices, system model, and the control algorithm), etc. [6]. In active control, the structural response under the input excitations are measured using sensors and an appropriate control force, calculated by a preassigned controller is used to drive the actuators for suppressing the unwanted structure vibrations.

Due to the popularity and importance of structural control, a number of textbooks [7, 8] and review papers have been presented. A brief review was presented by Housner et al. [2] in 1997, which discusses the passive, active, semi-active, and hybrid control systems and explores the potential of control theory in structural vibration control. It explains different types of control devices and sensors used in structural control. The paper concludes with some recommendations for future research.

A recent survey on active, semi-active, and hybrid control devices and some control strategies for smart structures were presented in [9, 10]. Some reviews were carried out with particular emphasis on active control [11–15], on semi-active control [16], and on control devices [17–19]. This shows that a significant progress has been made on most aspects of the structural control in the past few decades.

While there is no doubt about the advance, there still exist some areas which need more exploration. During the seismic excitation the reference where the displacement and velocity sensors are attached will also move, as a result the absolute value of the above parameters cannot be sensed. Alternatively, accelerometers can provide inexpensive and reliable measurement of the acceleration at strategic points on the structure. Most of the controllers use the displacement and velocity as its input variable, which are not easy to obtain from the acceleration signal with simple integration. Application of the state observers is impossible if the system parameters are unknown. Similarly, parameter uncertainty may be a problem for some control designs. There are different techniques available for identifying building parameters [20]. But these parameters may change under different load conditions. However, these control laws would be more applicable to real buildings if they could be made adaptive and robust to system uncertainty.

The active devices have the ability to add force onto the building structure. If the controller generates unstable dynamics, it can cause damage to the building. So it is important to study the stability of the controller. Only a few structural controllers such as H_∞ and sliding mode controller consider the stability in their design, whereas the other control strategies do not. Also, there is a lack of experimental verification of these controllers. Some other areas that demands attention are the time-delay present in the actuator mechanism, actuator saturation, and the optimal placement of sensors and actuators. The implementation of a controller will be challenging if these issues were not resolved. The motivation for the work presented in this book is to push forward the performance and capabilities of the structural vibration control system by acknowledging the above issues.

The objective of structural control system is to reduce the vibration and to enhance the lateral integrity of the building due to earthquakes or large winds, through an external control force [21]. In active control system, it is essential to design one controller in order to send an appropriate control signal to the control devices so that it can reduce the structural vibration. The control strategy should be simple, robust, fault tolerant, need not be an optimal, and of course must be realizable [22].

This chapter provides an overview of building structure modeling and control. It focuses on different types of control devices and control strategies used in structural control systems. This chapter also discusses system identification techniques and some important implementation issues, like the time-delay in the system, state estimation, and optimal placement of the sensors and control devices. A detailed version of this chapter can be found in [23].

2.2 Modeling of Building Structures

2.2.1 Models of Building Structures

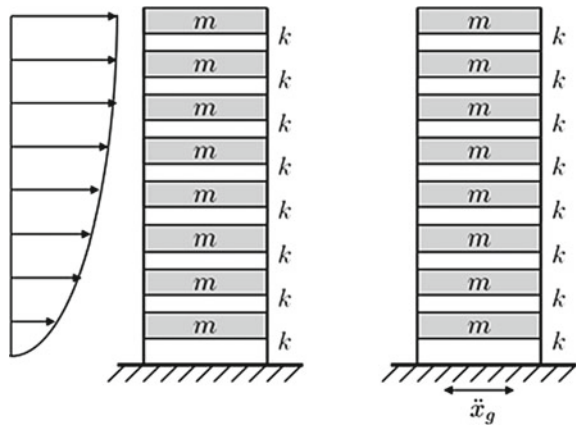
In order to derive a dynamic model of a building structure, it is important to know the behavior and impact of the excitations on the buildings, such as strong wind and seismic forces. The force exerted by the earthquake and wind excitation on the structure is shown in Fig. 2.1. An earthquake is the result of a sudden release of energy in the Earth crust that creates seismic waves. The building structure oscillates with the ground motion caused by these seismic waves and as a result the structure floor masses experience the inertia force. This force can be represented as

$$f = -m\ddot{x}_g \quad (2.1)$$

where m is the mass and \ddot{x}_g is the ground acceleration caused by the earthquake.

The movement of the structure depends on several factors like the amplitude and other features of the ground motion, the dynamic properties of the structure, the characteristics of the materials of the structure and its foundation (soil-structure interaction). A civil structure will have multiple natural frequencies, which are equal to its number of degree-of-freedom (DOF). If the frequency of the motion of the ground is close to the natural frequency of the building, resonance occurs. As a result, the floors may move rigorously in different directions causing inter-story drift, the relative translational displacement between two consecutive floors. If the building drift value or deformation exceeds its critical point, the building damages severely. Small buildings are more affected by high-frequency waves, whereas the large structures or high-rise buildings are more affected by low-frequency waves. The major part of the structure elastic energy is stored in its low order natural frequencies, so it is important to control the structure from vibrating at those frequencies [24].

Fig. 2.1 **a** Wind excitation;
b earthquake excitation



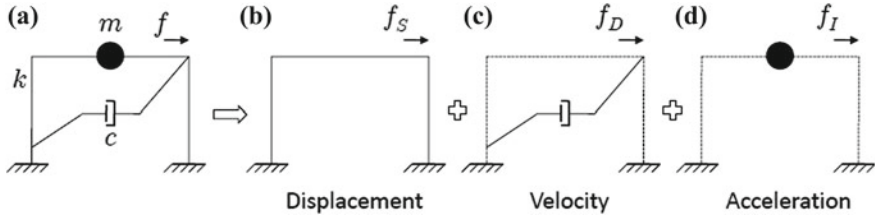


Fig. 2.2 a Structure; b stiffness component; c damping component; d mass component

In the case of high-rise flexible buildings, strong winds cause sickness or psychological responses like anxiety to the occupants and also may damage the fragile items. When the vibrations of taller buildings due to the high wind exceed a limit of 0.15 ms^{-2} , humans may feel uncomfortable [18]. As a result, the main objective of structural control is to reduce the acceleration response of buildings to a comfortable level. The force exerted by the wind on a building structure can be represented as [25];

$$F_w(h_i, t) = \Upsilon(h_i)v(t) \quad (2.2)$$

where $v(t)$ is the dynamic wind speed and $\Upsilon(h_i)$ has the following expression.

$$\Upsilon(h_i) = \rho_a \mu_p \mu_h \Delta_w(h_i) v_m \quad (2.3)$$

where ρ_a is the air density, μ_p is the wind pressure coefficient, $\Delta_w(h_i)$ is the windward area of the structure at elevation h_i , and v_m is the mean wind speed. The wind profile coefficient μ_h can be expressed as

$$\mu_h = (0.1h_i)^{2\alpha_a} \quad (2.4)$$

where α_a is a positive constant.

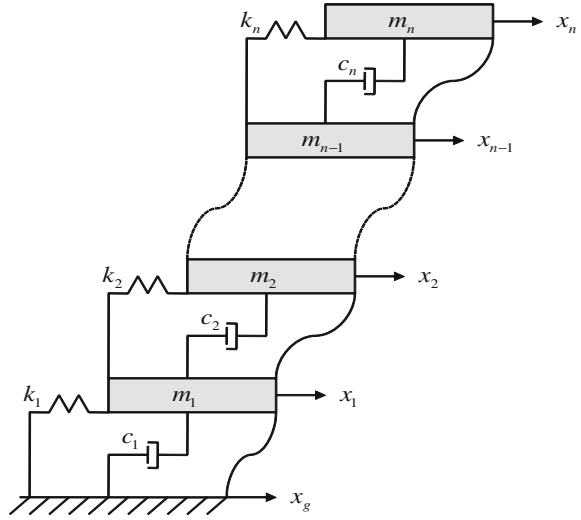
It is worth to note that the main difference between the effects of earthquake and wind forces on a structure is that, the earthquake causes internally generated inertial force due to the building mass vibration, whereas wind acts in the form of externally applied pressure.

A single-degree-of-freedom (SDOF) structure can be modeled using three components: the mass component m , the damping component c , and the stiffness component k [26], which is shown in Fig. 2.2. The stiffness component k can be modeled as either a linear or a nonlinear component, in other words elastic or inelastic, respectively [13]. Usually the mass is considered as a constant. When an external force f is applied to a structure, it produces changes in its displacement $x(t)$, velocity $\dot{x}(t)$, and acceleration $\ddot{x}(t)$.

Consider a simple building structure, which can be modeled by [26],

$$m\ddot{x} + c\dot{x} + kx = f_e \quad (2.5)$$

Fig. 2.3 Mechanical model of a n -DOF building structure



where m is the mass, c is the damping coefficient, k is the stiffness, f_e is an external force applied to the structure, and x , \dot{x} , and \ddot{x} are the displacement, velocity, and acceleration, respectively.

A model for a linear multistory structure with n -degree-of-freedom (n -DOF) is shown in Fig. 2.3. Here, it is assumed that the mass of the structure is concentrated at each floor. Neglecting gravity force and assuming that a horizontal force is acting on the structure base, the equation of motion of the n -floor structure can be expressed as [13],

$$M\ddot{\mathbf{x}} + C\dot{\mathbf{x}} + \mathbf{f}_s = -\mathbf{f}_e \quad (2.6)$$

For unidirectional motion, the parameters can be simplified as [13]:

$$M = \begin{bmatrix} m_1 & 0 & \cdots & 0 \\ 0 & m_2 & \cdots & \vdots \\ \vdots & \vdots & \ddots & \vdots \\ 0 & 0 & \cdots & m_n \end{bmatrix} \in \mathbb{R}^{n \times n}, \quad C = \begin{bmatrix} c_1 + c_2 & -c_2 & \cdots & 0 & 0 \\ -c_2 & c_2 + c_3 & \cdots & \vdots & \vdots \\ \vdots & \vdots & \ddots & \vdots & \vdots \\ \vdots & \vdots & \cdots & c_{n-1} + c_n & -c_n \\ 0 & 0 & \cdots & -c_n & c_n \end{bmatrix} \in \mathbb{R}^{n \times n}, \quad (2.7)$$

$\mathbf{x} \in \mathbb{R}^n$, $\mathbf{f}_s = [f_{s,1} \cdots f_{s,n}] \in \mathbb{R}^n$ is the structure stiffness force vector, and $\mathbf{f}_e \in \mathbb{R}^n$ is the external force vector applied to the structure, such as earthquake and wind excitations.

If the relationship between the lateral force \mathbf{f}_s and the resulting deformation \mathbf{x} is linear, then \mathbf{f}_s is

$$\mathbf{f}_s = K\mathbf{x}, \text{ where } K = \begin{bmatrix} k_1 + k_2 & -k_2 & \cdots & 0 & 0 \\ -k_2 & k_2 + k_3 & \cdots & \vdots & \vdots \\ \vdots & \vdots & \ddots & \vdots & \vdots \\ \vdots & \vdots & \cdots & k_{n-1} + k_n & -k_n \\ 0 & 0 & \cdots & -k_n & k_n \end{bmatrix} \in \Re^{n \times n} \quad (2.8)$$

If the relationship between the lateral force \mathbf{f}_s and the resulting deformation \mathbf{x} is nonlinear, then the stiffness component is said to be inelastic [26]. This happens when the structure is excited by a very strong force, that deforms the structure beyond its limit of linear elastic behavior. Bouc–Wen model gives a realistic representation of the structural behavior under strong earthquake excitations. The force-displacement relationship of each of the stiffness elements (ignoring any coupling effects) agrees the following relationship [27]:

$$f_{s,i} = \epsilon k_i x_i + (1 - \epsilon) k_i \eta \varphi_i, \quad i = 1 \cdots n \quad (2.9)$$

where the first part is the elastic stiffness and the second part is the inelastic stiffness, k_i is the linear stiffness defined in (2.8), ϵ and η are positive numbers, and φ_i is the nonlinear restoring force which satisfies

$$\dot{\varphi}_i = \eta^{-1} [\delta \dot{x}_i - \beta |\dot{x}_i| |\varphi_i|^{p-1} \varphi_i + \gamma \dot{x}_i |\varphi_i|^p] \quad (2.10)$$

where δ , β , γ , and p are positive numbers. The Bouc–Wen model has hysteresis property. Its input displacement and the output force is shown in Fig. 2.4. The dynamic properties of the Bouc–Wen model has been analyzed in [28].

In the case of closed-loop control systems, its input and output variables may respond to a few nonlinearities. From the control point of view, it is crucial to investigate the effects of the nonlinearities on the structural dynamics.

The Bouc–Wen model represented in (2.9) and (2.10) is said to be bounded input-bounded-output (BIBO) stable, if and only if the set Ω_{bw} with initial conditions $\varphi(0)$ is nonempty. The set Ω_{bw} is defined as: $\varphi(0) \in \Re$ such that f_s is bounded for all

Fig. 2.4 Hysteresis loop of Bouc–Wen model

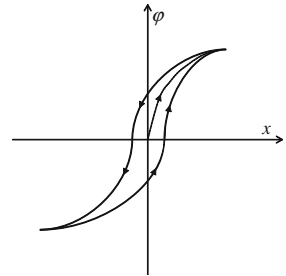


Table 2.1 Stability of Bouc–Wen model with different δ, β, γ .

Case	Conditions	Ω_{bw}	Upper bound of $ \varphi(t) $
1	$\delta > 0, \beta + \gamma > 0$ and $\beta - \gamma \geq 0$	\Re	$\max(\varphi(0) , \varphi_a)$
2	$\delta > 0, \beta - \gamma < 0$ and $\beta \geq 0$	$[-\varphi_b, \varphi_b]$	$\max(\varphi(0) , \varphi_a)$
3	$\delta < 0, \beta - \gamma > 0$ and $\beta + \gamma \geq 0$	\Re	$\max(\varphi(0) , \varphi_b)$
4	$\delta < 0, \beta + \gamma < 0$ and $\beta \geq 0$	$[-\varphi_a, \varphi_a]$	$\max(\varphi(0) , \varphi_b)$
5	$\delta = 0, \beta + \gamma > 0$ and $\beta - \gamma \geq 0$	\Re	$ \varphi(0) $
6	All other conditions	\emptyset	Unbounded

C^1 input signal, and x with fixed values of parameters δ, β, γ , and p , φ_a and φ_b are defined as

$$\varphi_a = \sqrt[p]{\frac{\delta}{\beta + \gamma}}, \varphi_b = \sqrt[p]{\frac{\delta}{\gamma - \beta}} \quad (2.11)$$

For any bounded input signal x , the corresponding hysteresis output f_s is also bounded. On the other hand if $\varphi(0) \in \Omega_{bw} = \emptyset$, then the model output f_s is unbounded. Table 2.1 shows how the parameter δ, β, γ , affect the stability property of the Bouc–Wen model.

In the case of n -DOF structures, the nonlinear model can be modified as

$$M\ddot{x}(t) + C\dot{x}(t) + F_s(x(t), \dot{x}(t)) = -M\Lambda\ddot{x}_g(t) \quad (2.12)$$

where $\Lambda \in \mathbb{R}^{n \times 1}$ denotes the influence of the excitation force.

2.2.2 Estimation and Sensing of Structure Parameters

Sensor and actuator placement. The optimal placement is concerned with placement of the sensing and controlling devices in preselected regions in order to closely perform the measurement and control operation of the structure vibration optimally. The actuator and sensor play an important role in deciding the system's controllability and observability, respectively. So it is important to perform an optimal placement of the sensors and actuators such that the controllability and observability properties of all or selected modes are maximized. Due to the above-mentioned reasons and importance, a number of studies are carried out about the optimal placements of devices [29, 30]. A survey on the optimal placement of control devices can be found in [10].

In [31], the actuator and sensor location performance index is calculated between the γ_{WZ}^2 and γ_{UY}^2 Hankel singular values. A nonnegative correlation coefficient κ is defined as

$$\kappa^2 = \frac{(\gamma_{WZ}^2)^T \gamma_{UY}^2}{\|\gamma_{WZ}^2\|_2 \|\gamma_{UY}^2\|_2} \quad (2.13)$$

where γ_{WZ}^2 and γ_{UY}^2 represents the Hankel singular values of the transfer functions G_{WZ} and G_{UY} , respectively. Here U and W are the inputs to the system and Y and Z are the outputs of the system. As per the above equation, the maximal performance is obtained with a better controllability and observability properties when κ reaches a maximal value; $\kappa = 1$, which is achieved when $\gamma_{UY}^2 = \gamma_{WZ}^2$.

A closed-loop optimal location selection method for actuators and sensors in flexible structures is developed by Guney et al. [30], which uses a simple H_∞ controller where the location optimization is performed using a gradient-based unconstrained minimization. Another related work is done in [32] using a H_2 norm-based computation for a reduced model of flexible structures, which considers only the dominant modes. They also proposed one GA for the nonlinear optimization problem for the reduced-order model. A GA is proposed in [33] through the formulation of a discrete and nonlinear optimization problem. Finally, the proposed algorithm is simulated for a 16-story building under 18 different earthquake excitations. In the work [25], it is concluded that the optimal position of actuators depends on the control algorithm, so that different control algorithms or different controllers yield different positions of the actuators.

Sensing. In order to identify the parameters of the civil structures, the dynamic response is studied from its input and output data, and the parameters are estimated using some sort of identification techniques. The inputs are the excitation forces like the earthquake and wind loads, and the outputs are the displacements, velocities, and accelerations corresponding to the input excitation. In practice, it is very difficult to derive an exact system model, so the original problem is to obtain parameters, such that the estimated model responses closely match the output of the building dynamic behaviors. There exists different methods for identification of both linear and nonlinear systems [34].

For the purpose of system identification, the structural system can be represented in many ways, such as ordinary differential equation (ODE), transfer functions, state-space models, and Auto Regressive Moving Average with exogenous input (ARMAX) models [35]. Consider a state-space variable $z = [x^T, \dot{x}^T]^T \in \mathfrak{R}^{2n}$, then the system described in (2.41) can be represented in state-space form as

$$\dot{z}(t) = Az(t) + Bu(t) + E\ddot{x}_g(t) \quad (2.14)$$

$$y(t) = Hz(t) + Du(t) \quad (2.15)$$

where $A \in \mathfrak{R}^{2n \times 2n}$, $B \in \mathfrak{R}^{2n \times n}$ and $E \in \mathfrak{R}^{2n}$.

$$A = \begin{bmatrix} 0 & I_n \\ -M^{-1}K & -M^{-1}C \end{bmatrix} \\ B = \begin{bmatrix} 0 \\ M^{-1}\Upsilon \end{bmatrix}, \quad E = \begin{bmatrix} 0 \\ -\theta \end{bmatrix}$$

Here, the matrices H and D and their dimensions change according to the design demands.

System identification can be broadly classified into parametric and nonparametric identification. In parametric identification, the system parameters like the mass, stiffness, and damping are estimated [36]. Most commonly used algorithms are least squares method, maximum likelihood method, extended Kalman filter, and variations of them [35]. Nonparametric identification determines a system model from the measured data, which is a mathematical function that can approximate the input-output representations sufficiently well [37]. This method is suitable for the systems with infinite number of parameters. Artificial neural network (ANN) is one of the popular nonparametric identification method [38]. Some other known methods are wavelet networks, splines, and neuro-fuzzy models [20].

Identification can also be classified into time-domain and frequency-domain, where the identification takes the form of time series and frequency response functions or spectra, respectively [20, 35]. System identification can be performed either using online or offline techniques. In offline identification, all the data including the initial states must be available before starting the identification process. For example, in the case of building parameter identification, the excitation and the corresponding structure response are recorded and later used for identification. Whereas, the online identification is done immediately after each input-output data is measured. In other words, the online identification is performed parallel to the experiment that is during the structural motion due to seismic or wind loads.

System identification of a linear MDOF structure under ambient excitation using the eigen space algorithm is presented in [39]. The algorithm identifies the damping and stiffness with known mass. In [40], two backpropagation neural networks (BPNN) are used to estimate the stiffness and damping of a 5-story building, where the first one is called emulator NN and the second one is known as the parametric evaluation NN. A modified GA strategy [41] and GA with gradient search [42] is proposed to improve the accuracy and computational time for parameter identification of MDOF structural systems. Sometime, the parameters are identified in the structure equipped with the actuator [6]. On the other hand, identification is performed only for the control devices. In [43], a memory-based learning called lazy recursive learning method based on NN is used to identify the MR damper behavior. The input current to the MR damper is varied and the corresponding damper behavior is modeled.

System identification is sometimes used for modal analysis, where the modal parameters like natural frequencies (ω_n) for different modes, modal shapes, and damping ratios (ζ) of the structures are estimated [20]. One such a simple technique is the analysis using Fourier transform techniques to estimate power spectra from which the modal parameters are estimated [35]. When the input excitation frequency equals the structure natural frequency, the magnitude of the vibration becomes higher. So it is important to estimate these low order natural frequencies and to control the structure from vibrating at those frequencies. A modified random decrement method along with Ibrahim time-domain technique is used for estimating the modal

parameters, which uses the floor acceleration [25]. The modal parameters can also be identified using Kalman filter [44].

Parametric identification of a linear structure excited with two orthogonal horizontal components using least-squares identification algorithm is presented in [45]. Here, each floor is considered to have 3-DOF, two displacements (along the x and y axis) and one torsion (rotation around the z axis). In [38], the dynamic state-space model of an earthquake-excited structure is identified using the measured input-output data that is used later for estimating the modal parameters. The system and modal parameters of a linear MDOF structure is estimated in [46]. Here, the equation of motion of the structure is first written in state-space equation of the observable canonical form and then is converted into an ARMAX model for dealing with the noise present in the measured data.

Some works [47] consider the damping matrix C as a Rayleigh damping coefficient matrix, which is found using the modal parameters as given below [26],

$$C = \alpha_R M + \beta_R K \quad (2.16)$$

where the Rayleigh parameters α_R and β_R are calculated using the first and third eigen-frequencies (ω_1 and ω_3), given by

$$\alpha_R = \frac{2\zeta\omega_1\omega_3}{\omega_1 + \omega_3} \text{ and } \beta_R = \frac{2\zeta}{\omega_1 + \omega_3} \quad (2.17)$$

whereas [24] uses the first two lower-order mode frequencies.

In [42], the stiffness of the structure column is estimated using the equation given below

$$k = \frac{12E_y I_m}{L_c^3} \quad (2.18)$$

where E_y is the Young's modulus of elasticity, I_m is the moment of inertia, and L_c is the unsupported length of the column.

A brief review about the identification of nonlinear dynamic structures is presented by Kerschen et al. [20] in 2006. The fundamentals and methods of identification for linear and nonlinear structural dynamic systems are reviewed in [35]. A general survey on system identification is presented in [48] and a review on stochastic identification methods for modal analysis is presented in [41].

Estimation of System States. In order to control the structural dynamics, it is necessary to measure the system states directly using a sensor or indirectly by using a state observer. Some structural control applications use Kalman filter as the observer for estimating the velocity and displacement [49]. A Kalman filter estimator is given by

$$\dot{\hat{z}} = A\hat{z} + Bu + L(y - H\hat{z} - Du) \quad (2.19)$$

$$L = R^{-1}(\gamma_g F E^T + HS)^T \quad (2.20)$$

where \hat{z} is the estimate of the state vector z , L is the Kalman filter gain matrix, S is the solution of the Algebraic Riccati equation using matrix R , and γ_g is the power spectral density of ground acceleration to the sensor noise. In [36], the Kalman–Bucy filter is used as the state estimator represented by

$$\dot{\hat{z}} = A\hat{z} + Bu + L(y - \hat{y}) \quad (2.21)$$

$$L = EC^T R^{-1} \quad (2.22)$$

Kalman filter cannot be applicable if the building parameters; mass, stiffness, and damping are not available, in that case sensors are used for the state estimation. There are different sensors available to measure displacement, velocity, and acceleration [2]. During the seismic excitation, the reference where the displacement and velocity sensors are attached will also move, as a result the absolute value of the above parameters cannot be sensed. Alternatively, accelerometers can provide inexpensive and reliable measurement of the acceleration at strategic points on the structure. A comparative study about the performance of the displacement, velocity, and acceleration sensors are performed in [3] and it is shown that the acceleration sensor is more effective compared to the other two sensors. A number of experiments and implementations about the acceleration feedback in structural control were carried out in [6].

An accelerometer measures the absolute acceleration, which is then integrated for estimating the velocity and displacement. Obtaining the velocity and displacement from the measured acceleration is a practically challenging task. Although time integration of the acceleration seems to be a straightforward solution for estimating the velocity and displacement, there are some practical difficulties that can result in a wrong estimation. Integrating these signals will result in the amplification of low frequencies components, reduction in the magnitude of high frequencies signals, and phase errors. In other words, the low-frequency signals including the DC offset present in the acceleration signal will dominate the result of the velocity and displacement, giving an unrealistic estimation.

The output of the accelerometer $a(t)$ can be expressed as

$$a(t) = k_a \ddot{x}(t) + \varphi(t) + \varepsilon \quad (2.23)$$

where k_a is the accelerometer gain, $\varphi(t)$ is the noise and disturbance effects of the measurement, and ε denotes the DC bias [42]. Accelerometer has different source of noise, integrating these noise signals leads to an output that has a root mean square (RMS) value that increases with integration time, even in the absence of any motion of the accelerometer [50]. The RMS positional error $e_{x(t)}$ of an acceleration signal with a bias ε can be approximated as

$$\text{RMS}\{e_{x(t)}\} = \frac{1}{2} \varepsilon t^2 \quad (2.24)$$

which will grow at a rate of t^2 .

It has been shown that the aliasing can cause low-frequency errors in the measured acceleration signal [51]. Aliasing is an unavoidable phenomenon that happens when digitizing the analog signals using an analog-to-digital converter (ADC). During this conversion, the frequency components above the Nyquist rate are folded back into the bandwidth of interest. Then, the acceleration signal in (2.23) can be rewritten as

$$a(t) = k_a \ddot{x}(t) + \varphi(t) + \varepsilon + \ddot{x}_s(t) \quad (2.25)$$

where $\ddot{x}_s(t)$ is the aliasing content due to sampling. This low-frequency content will be amplified during the integration process. This aliasing effect is not completely removable but its effect can be minimized by using an anti-aliasing filter between the accelerometer and data acquisition card. The ADC sampling rate needs to be high enough compared to this filter cutoff frequency and the sampling should be done in uniform time intervals.

The other source of offset in the measured acceleration is the ADC itself [43]. If the acceleration is slow compared with the quantization level of the conversion, an offset is added into the acceleration signal. This effect can be reduced by increasing the resolution of the ADC.

Apart from these issues, the integration output can also be affected by the integration techniques. The integration methods like the Trapezium rule, Simpson's rule, and Tick's rule have problems with low-frequency components, and they also show instability at high frequencies [52].

A drift-free integrator is proposed by Gavin et al. [53], which is implemented using analog and digital circuits. The paper presents three types of integrators: (1) implemented using a first order low-pass filter as the integrator and two stages of high-pass filters for removing the offset, (2) analog integrator with feedback stabilization, and (3) a stabilized hybrid analog–digital integrator with an exponential accuracy when integrating long-period signals. In another work [54], the drift due to the integration is eliminated by; first filtering the acceleration signal using a frequency-domain filter called Fast Fourier transform-direct digital integration (FFT-DDI) and then is integrated for estimating the velocity and displacement. The same method is repeated for removing the drift occurred due to the unknown initial conditions.

The constant offset present in the acceleration data can be represented using a baseline. The integration may cause a drift in this baseline, which will give a wrong estimation. A baseline correction method is proposed in [55] that uses a least-square curve fitting technique and a frequency-domain filtering for avoiding the drift during the integration. The correction is done by determining a baseline in polynomial form, which is then subtracted from the measured acceleration signal, then is integrated to obtain the velocity and displacement. Finally, a windowed filter is applied to remove the low-frequency noise.

A practical method for calibrating the positional error obtained by double integrating the acceleration signal is discussed in [50]. The double integration of noise using different techniques is also presented. An initial velocity determination method for the displacement estimation from the acceleration data is suggested in [56], which also considers the initial condition in their design. A weighted residual parabolic

acceleration time integration method is proposed in [57], where the displacement is assumed to be a fourth-order polynomial, so that the acceleration variation with time is quadratic. A numerical integrator for estimating the velocity and displacement from the measured acceleration signal is proposed in [23]. The effectiveness of the integrator is illustrated experimentally by performing a structural vibration control on a shake table using a PD controller.

2.3 Structural Control Devices

The structural vibration control is aimed to prevent structural damages using vibration control devices. Various control devices have been developed to ensure the safety of the building structure even when excessive vibration amplitudes occur due to earthquake or wind excitations. The control devices are actuators, isolators, and dampers, which are used to attenuate the unwanted vibrations in a structure. Many active and passive devices have been used as vibration control devices. The passive damper modifies the structure response without using an external power supply. Active actuators can generate required forces for controlling the structure dynamics. Using an external power supply, these devices will modify the structure stiffness or damping, which results in a structural dynamics change. The semi-active device combines the properties of both passive and active devices. Hybrid devices are formed either by using both passive and active devices or by using both passive and semi-active devices. Other well-known vibration control devices are the base isolators. The list of the commonly used structural control devices is summarized in the Table 2.2. Basic concepts of some popular devices are discussed below.

Table 2.2 Structural control devices [7, 17, 19]

Passive	Active	Semi-active	Isolator	Hybrid
TMD, TLCD, metallic dampers, friction dampers, viscoelastic dampers, viscous fluid dampers	AMD, active tendons	MR/ER dampers, semi-active TMD, semi-active TLCD, friction control devices, stiffness control devices, viscous fluid dampers	Elastomeric bearings, lead-plug bearings, high-damping rubber bearings, friction pendulum bearings	HMD, HBI

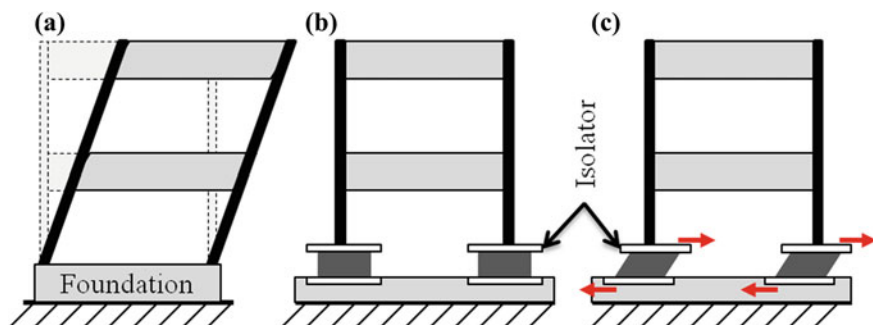


Fig. 2.5 Base isolation system

2.3.1 Base Isolators

Base isolators are flexible isolation devices, placed between the building structure and the foundation for reducing seismic wave propagation into the structure. The addition of this device will increase the flexibility of the structure, hence, the structural time period. For that reason, isolators reduce the propagation of high frequency signal from ground to the structure, which makes it suitable for implementing in small and middle-rise building structures [7]. The Fig. 2.5 shows the changes in the structure response while using base isolator.

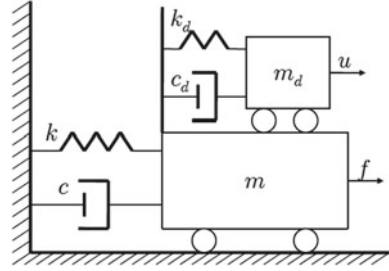
Base isolation is one of the popular technique applied widely, especially in the case of bridges. In general, the isolators can be formed using elastomeric bearings, sliding bearings, and combinations of both types of bearings. Elastomeric bearings are made up of elastic materials like the rubber. In the second case, the isolator uses sliding mechanism [7]. In bridges, the isolators are easily implemented by replacing standard bridge bearings by isolation bearings. More information about the types of isolators and their implementation can be found in [58].

Base isolation is well-known passive control technique. But active [59] and semi-active [60] control schemes were also proposed. Another class of base isolation devices is the hybrid base isolation (HBI), made by combining the passive base isolator with the active or semi-active base isolator/control [18]. Sometimes, the seismic activity in the building is reduced by placing isolators between the substructure columns, not in the base, hence called as seismic isolators.

2.3.2 Passive Devices

Structural control using passive devices is called passive control. A passive control device does not require an external power source for its operation and utilizes the motion of the structure to develop the control forces. These devices are normally termed as energy dissipation devices, which are installed on structures to absorb a

Fig. 2.6 Mechanical model of Building-TMD



significant amount of the seismic-or wind-induced energy. The energy is dissipated by producing a relative motion within the control device with respect to the structure motion [19]. For the ideal passive devices, the control forces applied to the structure are only dependent to the structural motion, which can be mathematically represented as [6]

$$f_i(t) = -c_i \dot{x}_{di}(t) \quad (2.26)$$

where \dot{x}_{di} is the relative velocity across the i th device and c_i is the damping coefficient associated with the i th device.

Vibration absorber systems such as tuned mass damper (TMD) has been widely used for vibration control in mechanical systems. Basically, a TMD is a device consisting of a mass attached to a building structure such that it oscillates at the same frequency of the structure, but with a phase shift. The mass is usually attached to the building through a spring-dashpot system and energy is dissipated by the dashpot as relative motion develops between the mass and structure [61]. A simple mechanical model for TMD is depicted in Fig. 2.6. An early study about the TMD with a practical application is illustrated in [62].

Tuned liquid column damper (TLCD) dissipates energy similar to that of TMD, where the secondary mass is replaced with a liquid column, which results in a highly nonlinear response. They dissipate energy by passing the liquid through the orifices. A simple mechanical model of TLCD is depicted in Fig. 2.7. The natural frequency of the TLCD can be obtained as [63]

$$\omega_n = \sqrt{\frac{2g}{L_t}} \quad (2.27)$$

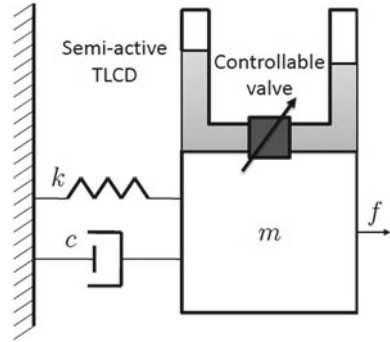
where L_t is the length of the liquid tube and g is the acceleration due to gravity.

The equation of motion of a TLCD satisfies the following expression [64]

$$\rho_l \Delta L_t \ddot{x}_v(t) + \frac{1}{2} \rho_l \Delta \xi |\dot{x}_v(t)| \dot{x}_v(t) + 2 \rho_l \Delta g x_v(t) = -\rho_l \Delta L_h \ddot{x}(t) \quad (2.28)$$

where $x_v(t)$ is the vertical displacement, ρ_l is the liquid density, L_h and L_t , respectively are the horizontal and total length of the liquid column, Δ is the area of cross

Fig. 2.7 Mechanical model of TLCD



section, and ξ is the headless coefficient. A comparison study of the performance of three types of mass dampers; TMD, TLCD, and Liquid column vibration absorber (LCVA) were discussed in [59] and it is concluded that the TMD performs better than the other two dampers.

Other passive dampers are [17]: metallic yield dampers which dissipate the energy through the inelastic deformation of metals, friction dampers which utilize the mechanism of solid friction, develops between two solid bodies sliding relative to one another, to provide the desired energy dissipation, and viscoelastic dampers that dissipates the energy through the shear deformation.

Viscous fluid damper works based on the concept of sticky consistency between the solid and liquid. It has a movable piston within a housing filled with highly viscous fluid. The piston contains a number of orifices, through which the fluid passes from one side to another that will result in energy dissipation. The output force of the orifice controlled viscous fluid devices can be expressed as [65]

$$f(t) = c |\dot{x}_d(t)|^{\alpha_c} \text{sgn}(\dot{x}_d(t)) \quad (2.29)$$

where \dot{x}_d is the relative velocity of the viscous fluid device and α_c is a coefficient in the range of 0.3–2.0.

Passive dampers are very simple and due to the fact that it will not add energy to the structure, hence it cannot make the structure unstable. Most of the passive dampers can be tuned only to a particular structural frequency and damping characteristics. Sometimes, these tuned values will not match with the input excitation and the corresponding structure response. For example; (1) nonlinearities. in the structure cause variations in its natural frequencies and mode shapes during large excitation, (2) a structure with a multiple-degree-of-freedom (MDOF) moves in many frequencies during the seismic events. As the passive dampers cannot adapt to these structure response changes, it cannot assure a successful vibration suppression [9]. This is the major disadvantage of the passive dampers, which can be overcome by using multiple passive dampers, each tuned to different frequencies (e.g., doubly TMD, Multiple TMD) or by adding an active control to it.

2.3.3 Active Devices

The concept of active control has started in early 1970s and the full-scale application was performed in 1989 [18]. An active control system can be defined as a system that typically requires a large power source for the operation of electrohydraulic or electromechanical (servo motor) actuator, which increases the structural damping or stiffness. The active control system uses sensors for measuring both the excitation and structural responses, and actuators for controlling the unwanted vibrations [19]. The working principle of the active control system is that, based on the measured structural response the control algorithm will generate control signal required to attenuate the vibration. Based on this control signal, the actuators placed in desired locations of the structure generate a secondary vibrational response, which reduces the overall structure response [66]. Depending on the size of the building structure, the power requirements of these actuators vary from kilowatts to several megawatts [67]. Hence, an actuator capable of generating a required control force should be used. As the active devices can work with a number of vibration modes, it is a perfect choice for the MDOF structures. A number of reviews on active structural control were presented [11].

The ideal actuators are assumed to have the ability to instantaneously and precisely supply force commanded by the control algorithm [6]. There are many active control devices designed for structural control applications. A recent survey on active control devices is presented in [9]. An active mass damper (AMD) or active tuned mass damper (ATMD) is created by adding an active control mechanism into the classic TMD. In this system, 1 % of the total building mass is directly excited by an actuator with no spring and dashpot attached. ATMD control devices were first introduced in [68]. These devices are initially used to reduce structural vibrations under strong winds and moderate earthquake.

Active tendons are prestressed cables, where its stress is controlled using actuators for suppressing the vibration [9]. The structural vibration control using active cables and tendons is presented in [12]. Various numerical analytical studies have been carried out using tendons for active control [69]. At low excitations, the active control system can be switched-off, then the tendons will resist the structural deformation in passive mode. At higher excitations, active mode is switched-on to reach the required tension in tendons.

A comparison study between active and passive control systems was carried out in [6] using H_2/LQG control algorithm. In simulation, it is found that for SDOF structure both the active and passive control systems performed similarly, whereas in the case of structure with MDOF the active control system showed high performance.

The active control devices found to be very effective in reducing the structural response due to high magnitude earthquakes. However, there are some challenges left to the engineers, such as how to eliminate the high power requirements, how to reduce the cost, and maintenance. These challenges resulted in the development of semi-active and hybrid control devices [70].

2.3.4 Semi-active Devices

A semi-active control system typically requires a small external power source for its operation and utilizes the motion of the structure to develop control force, where the magnitude of the force can be adjusted by an external power source [19]. It uses the advantages of both active and passive devices. The semi-active devices for structural control application were first proposed by Hrovat et al. in 1983 [71].

The benefits of the semi-active devices over active devices are their less power requirements, which can even be powered using a battery that is more important during the seismic events, when the main power source to the building may fail. Semi-active devices cannot inject mechanical energy into the controlled structural system, but has properties that can be controlled to optimally reduce the response of the system. Therefore, in contrast to active control devices, semi-active control devices do not have the potential to destabilize (in bounded-input bounded-output sense) the structural system [70]. A detailed review of semi-active control systems is provided in [72].

Like passive friction dampers, these semi-active frictional control devices dissipate energy through friction caused by the sliding between two surfaces. For this damper, a pneumatic actuator is provided in order to adjust the clamping force [73]. An ideal friction damper can be modeled as a Coulomb element, where the output force is termed as

$$f = \mu f_n \operatorname{sgn}(\dot{x}) \quad (2.30)$$

where μ is the friction coefficient and f_n is the normal force [19]. In the case of friction dampers, the friction coefficient needs to be tuned to have a good energy dissipation. In contrast with the passive friction dampers, the semi-active friction dampers can easily adapt the friction coefficient to varying excitations from weak to strong earthquakes.

Semi-active controllable fluid dampers are one of the most commonly used semi-active control device. For these devices, the piston is the only moving part, which makes them more reliable. These devices have some special fluid, where its property is modified by applying external energy field. The electric and magnetic fields are mainly used to control these devices, which is so-called as Electro rheological (ER) and magneto rheological (MR) dampers, respectively [17].

ER damper [19]: ER dampers consist of liquid with micron-sized dielectric particles within a hydraulic cylinder. When an electric field is applied, these particles will polarize due to the aligning, thus offers more resistance to flow resulting a solid behavior. This property is used to modify the dynamics of the structure to which it is attached.

MR damper [19]: The construction and functioning of MR dampers are analogous to that of ER dampers, except the fact that instead of the electric field, magnetic field is used for controlling the magnetically polarizable fluid. MR dampers have many advantages over ER dampers, which made them more popular in structural control applications. These devices are able to have a much more yield stress than ER with less

Table 2.3 MR and ER damper properties

Property	MR damper	ER damper
Max. yield stress	50–100 kPa	2–5 kPa
Maximum field	~250 kA/m	~4 kV/mm
Plastic viscosity	0.1–1.0 Pa-s	0.1–1.0 Pa-s
Operable temperature range	–40 to 150 °C	+10–90 °C
Stability	Unaffected by most impurities	Cannot tolerate impurities
Response time	milliseconds	milliseconds
Density	3–4 g/cm ³	1–2 g/cm ³
Maximum energy density	0.1 J/cm ³	0.001 J/cm ³
Power supply (typical)	2–25 V; 1–2 A	2000–5000 V; 1–10 mA

input power. Moreover, these devices are less sensitive to impurities. A comparison between MR and ER fluid dampers are summarized in Table 2.3.

Different modeling techniques are available to express the behavior of these devices, such as; Bingham model, Bingham viscoplastic model, Gamota and Filisko model, Bouc–Wen model, modified Bouc–Wen model, etc. [74]. Among these techniques, Bingham model is the simplest modeling tool for both ER and MR dampers. When any field is applied to these devices, the change in the fluid property can be modeled using a Bingham viscoplastic model [12]. The plastic viscosity of this model is given in terms of the shear stress and shear strain, which is mathematically represented as

$$\tau = \tau_y \operatorname{sgn}(\dot{\gamma}) + \eta \dot{\gamma} \quad (2.31)$$

where τ is the total shear stress, τ_y is the yield stress due to the applied field, $\dot{\gamma}$ is the rate of the shear strain, and η is the plastic viscosity. The relationship between the force and displacement of a MR damper using this model is given by [75]

$$f = \frac{12\eta_N L_p \Delta_p^2}{\pi D_i D_p^3} \dot{x}(t) + \frac{3L_p \tau_y}{D_p} \Delta_p \operatorname{sgn}[\dot{x}(t)] \quad (2.32)$$

where L_p is the piston length, Δ_p is the piston cross-sectional area, D_i is the inner diameter, D_p is the diameter of the small gap in the piston, and η_N is the Newtonian viscosity independent of the applied magnetic field. The yield stress can be represented as a function of the control current I as follows.

$$\tau_y = A_1 e^{-I} + A_2 \ln(I + e) + A_3 I \quad (2.33)$$

where A_1 , A_2 and A_3 are the coefficients relative to the MR fluid property and e is the Euler's number.

Bingham model is a mechanical version of the Bingham viscoplastic model, which uses damping and Coulomb friction components in the model. This model is further extended, known as Gamota and Filisko model, which is a parametric

viscoelastic-plastic model. But all of these methods have some shortcomings especially at low velocities. The classic Bouc–Wen can model the hysteresis loop pretty well, but fails to predict the roll-off problem seen at low velocities. A modified Bouc–Wen model was proposed by Spencer et al. [74], where an additional damping (c_1) and stiffness (k_1) is added to compensate the roll-off and accumulator stiffness, respectively. The total force of the MR damper is obtained as

$$\begin{aligned} f &= \alpha_b \tilde{z} + c_0(\dot{x} - \dot{\tilde{y}}) + k_0(x - \tilde{y}) + k_1(x - x_0) \\ &= c_1 \dot{\tilde{y}} + k_1(x - x_0) \end{aligned} \quad (2.34)$$

where \tilde{y} and \tilde{z} can be found as

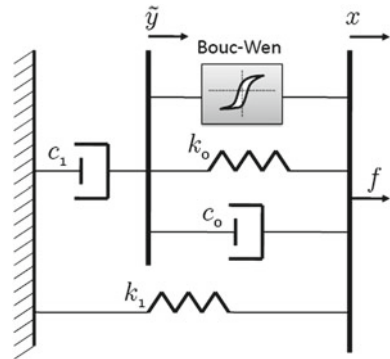
$$\dot{\tilde{z}} = -\gamma_m \left| \dot{x} - \dot{\tilde{y}} \right| \tilde{z} |\tilde{z}|^{\tilde{n}-1} - \beta_m \left(\dot{x} - \dot{\tilde{y}} \right) |\tilde{z}|^{\tilde{n}} + \delta_m \left(\dot{x} - \dot{\tilde{y}} \right) \quad (2.35)$$

$$\dot{\tilde{y}} = \frac{1}{c_0 + c_1} \{ \alpha_b \tilde{z} + c_0 \dot{x} + k_0(x - \tilde{y}) \} \quad (2.36)$$

where c_0 is the viscous damping at large velocities, c_1 is the viscous damping for force roll-off at low velocities, k_0 is the stiffness at large velocities, k_1 is the damper accumulator stiffness, and x_0 is the initial displacement of spring. k_1 and α_b is a third-order polynomial. The corresponding mechanical model is depicted in Fig. 2.8. In [55], the dynamic modeling and two quasi-static models (axisymmetric and parallel-plate model) of the MR damper are studied through experiments.

The semi-active fluid viscous damper consists of a hydraulic cylinder, which is separated using a piston head. The cylinder is filled with a viscous fluid, which can pass through the small orifices. An external valve which connects the two sides of the cylinder is used to control the device operation. The semi-active stiffness control device modifies the system dynamics by changing the structural stiffness [19].

Fig. 2.8 Modified Bouc–Wen model of MR damper



2.3.5 Hybrid Devices

Hybrid actuators combine robustness of the passive device and high performance of the active devices. Due to the inclusion of multiple control devices, the hybrid system overcomes the limitations and restrictions seen in the single control devices like passive, active, and semi-active devices. The hybrid systems are further classified into two classes: HBI and hybrid mass damper (HMD) [18]. As the base isolation exhibits nonlinear behavior, various nonlinear control technologies like the robust control were adopted to control these hybrid devices [70].

HMD can be formed by combining the passive devices like TMD along with some active devices like AMD. The capability of the TMD is increased by adding a controlling actuator to it, which increases the system robustness in changing the structure dynamics. These HMDs are found to be cost effective in terms of the energy requirement for their operation, when compared with active control systems [18]. The full-scale implementation of active structural control systems in Japan, USA, Taiwan, and China are enlisted in [17], where the HMD is found to be the most commonly employed device compared with other devices.

Researchers have also investigated the various control methods for HMD, like optimal control methods, sliding mode control, gain scheduling, etc. [70]. As these systems utilize two types of actuators, it will have a series of objective functions, which results in a multi-objective optimization problem. To derive an optimal solution, a preference-based optimization model using GA is proposed. The designed model is compared with a non-hybrid system and is found to be very cost effective in suppressing the vibrations. A hybrid system using the HMD and a viscous damper is discussed in [76] for the reduction of the wind-induced vibrations of high-rise building.

The implementation of the above-mentioned devices will result in different control schemes, which are summarized in Fig. 2.9. In the passive control, the passive device reduces the vibration response of a structure without using any feedback, see Fig. 2.9b. In the active and semi-active case, the input and output response of the structure is measured and based on that the controller generates a desirable output command signal. This signal is then used to drive the active or semi-active devices for attenuating the vibration, which are shown in Fig. 2.9c, d, respectively. In the case of hybrid control shown in Fig. 2.9e, only the active/semi-active device uses the feedback, whereas the passive devices work independently.

Typical installations of control devices are shown in Fig. 2.10. Other recent technique is the connected control method, where the adjacent buildings are interconnected using control devices for vibration attenuation, see Fig. 2.11. In [77], passive devices are installed between the adjacent structures for inter-structure protection and at the same time semi-active dampers are placed in the building floors for protecting the substructure.

A brief state-of-the-art review about the structural control devices can be found in [17]. The simplicity of the passive systems made them more common in seismic control applications. The active systems including the semi-active and hybrid systems,

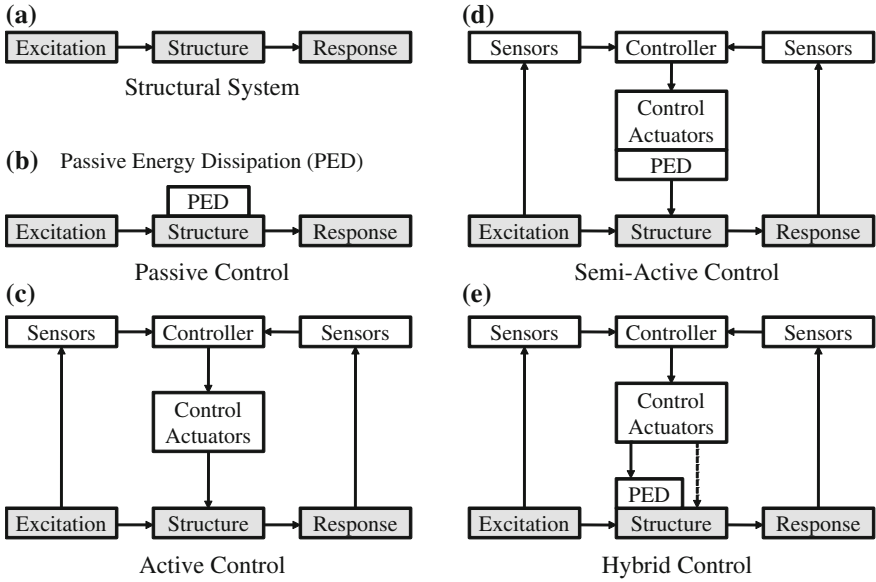


Fig. 2.9 Control schemes [17]

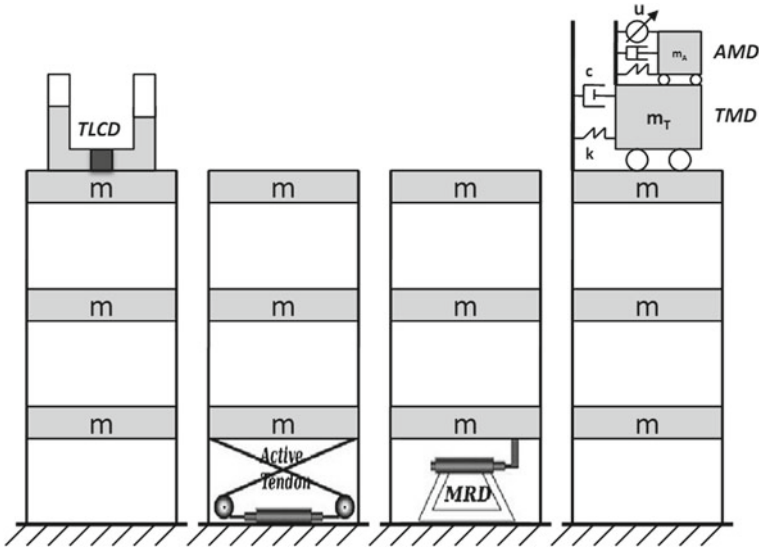
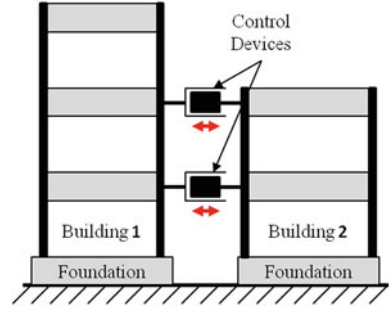


Fig. 2.10 Typical implementation of control devices on structures

generates a control force based on the measurements of the structural responses. Due to this ability of measuring the structural response it can be designed to accommodate a variety of disturbances, which makes them to perform better than the passive systems. More on the governing equations of dampers and actuators can be found in [47].

Fig. 2.11 Buildings interconnected using dampers



Control devices are used to control the dynamics of the structure to a desired response. Therefore, the dynamic model of a structure will change once a control device is installed on it. That is, it is expected that the installation of a control device will modify the structure parameters like its natural frequency, thereby changing the system model [36]. As a consequence, it is necessary to consider the dynamics of the actuator in the structure.

Consider a passive damper added to a structure represented in (2.37), then the system model can be rewritten as [17]

$$m\ddot{x} + c\dot{x} + kx + \Pi(x) = -(m + m_d)\ddot{x}_g \quad (2.37)$$

where m_d is the mass of the damper and $\Pi(x)$ represents the force corresponding to the damper, used to modify the structure response for reducing vibrations. The same formulation can be done in the case of active control devices, where (2.37) can be rewritten as follows

$$m\ddot{x} + c\dot{x} + kx = -mu(t) - m\ddot{x}_g \quad (2.38)$$

If the control force is selected as per the relationship given in (2.39)

$$u(t) = \frac{\Pi(x)}{m} \quad (2.39)$$

then (2.38) becomes

$$m\ddot{x} + c\dot{x} + kx + \Pi(x) = -m\ddot{x}_g \quad (2.40)$$

In contrast to the passive control method, here, the control function $\Pi(x)$ is derived as a control law.

The motion equation of a structural system with n -DOF and o control devices subjected to an earthquake excitation can be expressed as

$$M\ddot{x}(t) + C\dot{x}(t) + Kx(t) = \Gamma u(t) - M\Lambda\ddot{x}_g(t) \quad (2.41)$$

where $u(t) \in \mathbb{R}^{n \times 1}$ is the control force vector and $\Gamma \in \mathbb{R}^{n \times o}$ is the location matrix of the control devices. Equation (2.41) becomes nonlinear if the control force is generated using a nonlinear device, such as MR damper or by using a nonlinear control algorithm, such as intelligent control.

2.4 Active Structural Control Techniques

The objective of structural control system is to reduce the vibration and to enhance the lateral integrity of the building due to earthquakes or large winds, through an external control force [21]. In active control system, it is essential to design one controller in order to send an appropriate control signal to the control devices so that it can reduce the structural vibration. The control strategy should be simple, robust, fault tolerant, need not be an optimal, and of course must be realizable [22].

2.4.1 Linear Control of Building Structures

PID Control. The proportional-integral-derivative (PID) has been widely conducted for practical applications, especially for the systems with one or two DOF. For multivariable systems, its control algorithm becomes more complex, which makes them unsuitable for the applications like vibration control of MDOF flexible structures. A simulation was carried out for a simple proportional controller, which is able to reduce the building displacement for wind excitation, but found to be ineffective for strong earthquake excitation [13].

In [78], two PD controllers were used for controlling two actuators installed in the first and fifteenth floor. The control law is given as

$$u(t) = K_p \left[e(t) + K_d \frac{de(t)}{dt} \right] \quad (2.42)$$

where K_p and K_d are the proportionality constant and derivative time, respectively, and $e(t)$ is the position error. The designed PD controller performance is found to be less efficient when compared with that of a fuzzy logic controller (FLC).

In a work done by [79], a PID controller is designed which have the following controlling law

$$u(t) = K_p \left[e(t) + \frac{1}{K_i} \int_0^t e(t)dt + K_d \frac{de(t)}{dt} \right] \quad (2.43)$$

where K_i is the integral gain. Here, the PID performance is compared with that of a sliding mode controller (SMC) and found to be less effective in controlling the structural vibration. In [80], a proportional-integral (PI) controller is used to actuate the AMD against the structural motion due to earthquake.

H_∞ Control. H_∞ technique is one of the widely used linear robust control scheme in structural vibration control. This technique is insensitive with respect to the disturbances and parametric variations, which makes them suitable for the MIMO type structural control systems [81].

A modified H_∞ controllers, for example, pole-placement H_∞ control is presented in [76]. In this work, instead of changing the structure stiffness some target damping ratio is considered. A bilinear transform is adopted to locate the closed-loop poles in a specific region within the H_∞ controller design framework. The relation between the final closed-loop poles and bilinear transform parameters is derived as a quadratic equation and using this equation a new noniterative direct method is developed for an optimal H_∞ controller design.

Normally, the H_∞ design results in a higher order system, which will make the implementation more difficult [62]. So it may be necessary to reduce its order, which can be done by performing balanced truncation. The truncation has two classes; direct method and indirect method. The balanced truncation assures very few information losses about the system, which is achieved by truncating only less controllable and observable states. It is shown that the performance of the reduced low order system is nearly same as the performance of the actual higher order controller.

A H_∞ based structural controller using Takagi–Sugeno Fuzzy model was proposed in [82]. The controller stability is derived based on Lyapunov stability theory, which is evaluated as a LMI problem. If the initial condition is considered, the H_∞ control performance satisfies the following condition:

$$\int_0^{t_f} z^T(t) Q z(t) dt \leq z^T(0) P z(0) + \epsilon^2 \int_0^{t_f} \ddot{x}_g^T \ddot{x}_g dt \quad (2.44)$$

where t_f denotes the termination time of the control, P and Q are the positive definite matrices, and ϵ denotes the effect of \ddot{x}_g on $z(t)$. The effectiveness of the proposed algorithm is demonstrated through numerical simulations on a 4-story building.

As discussed earlier, time-delay is an important factor to be considered while designing a control system. A H_∞ controller is presented in [83], which considers time-delay in control input u . The proposed algorithm determines the feedback control gain with a random search capability of GA and solving a set of LMIs. The effectiveness of the proposed algorithm is proved through simulation of a system with larger input time-delay.

Optimal Control. Optimal control algorithms are based on the minimization of a quadratic performance index termed as cost function, while maintaining a desired system state and minimizing the control effort [13]. The most basic and commonly used optimal controller is the linear quadratic regulator (LQR). For structural control applications, the acceptable range of structure displacement and acceleration are considered as the cost function that is to be minimized.

An energy-based LQR is proposed in [69], where the controller gain matrix is obtained by considering the energy of the structure. The structural energy is defined as

$$\frac{1}{2}\dot{x}^T(t)M\dot{x}(t) + \frac{1}{2}x^T(t)Kx(t) \quad (2.45)$$

where the first term is the kinetic energy and the second term is the potential energy of the structural system.

A modified LQR is proposed in [4], which is formed by adding an integral and a feedforward control to the classic LQR. A state feedback gain and an integral gain are used to reduce the steady-state error. A feedforward control is included to suppress the structural responses and to reduce the effect of earthquakes. A structural vibration control utilizing a filtered LQ control is presented in [84]. As all the structural state variables are not observable, a suboptimal control is used, where the system states are reduced using low-pass filters. A LQR based on GA is presented [24], where the GA is used for choosing the weighting matrix.

Sometime, states of the structures are measured indirectly using some observers like Kalman filters. The addition of a Kalman filter to a LQR control strategy leads to what is termed as Linear Quadratic Gaussian (LQG) [36]. In other words, LQG is formed by combining the linear quadratic estimator with LQR. These LQG are generally used for the systems which has Gaussian white noise [10].

The conventional LQG controller sometimes do not consider the input force term in their design. Chen [82] proposed an active vibration control scheme using a combination of LQG and an input estimation approach. The input estimation approach is introduced to observe the input disturbance forces for the open loop control, that is used to cancel out the input forces. The proposed method is evaluated through numerical experiments on linear lumped-mass systems and a better performance is reported compared to that of the conventional LQG.

An active controller utilizing MR damper is designed using LQG control strategy under a wind loading by means of drag forces [36]. A real set of recorded wind speed data is used to excite the laboratory prototype. A H_2 /LQG based controller is presented in [33], which uses wireless sensing motes (MICA2) for sensing the acceleration signal. More works about the structural control using LQR/LQG control algorithms can be found in [85]. Optimal algorithms based on instantaneous optimal control has also been developed for nonlinear systems. The nonlinear optimal methods using GA, FLC, etc., will be discussed later.

2.4.2 Intelligent Control of Building Structures

Neural Network Control. In recent years, the structural control systems based on NN are very popular, because of its massively parallel nature, ability to learn, and its potential in providing solutions to the foregoing unsolved problems. They provide a general framework for modeling and control of nonlinear systems such as building structures.

In the middle of the 1990s, very few structural control applications have been reported based on NN. Wen et al. [86] presented a NN-based active control of a

SDOF system that can become nonlinear and inelastic. One inverse mapping NN and one emulator NN are used in the design. The difference between the actual overall structural response and response due to the control force only, is used as the input to the inverse mapping NN. The emulator NN predicts the response of the structural system to the applied control force. Using this response, a control force with a phase shift is generated to nullify the excitation.

A backpropagation (BP)-based ANN for active control of SDOF structure is proposed by Tang [22]. This control strategy does not need the information of the external excitation in advance and the control force needed for the next sampling time is completely determined from the currently available information. The ANN with five neuron elements (displacement, velocity, and load of the preceding time step and displacement and velocity of the current time step) is used, which will perform two sequential calculations in every sampling interval; (a) calculate the load (b) based on the calculated load, the control force $u(t)$ needed for the next time interval is calculated. Apart from the numerical verification of the above algorithm, they have also presented a study on the uncertainties in the system modeling and input motion.

Consider the minimization of the cost function in a discrete form with total time step r and increment time Δt

$$\hat{J} = \sum_{\hat{n}=0}^r \hat{J}_{\hat{n}} = \frac{1}{2} \sum_{\hat{n}=0}^r (z[\hat{n}]^T Q z[\hat{n}] + u[\hat{n}]^T R u[\hat{n}]) \Delta t \quad (2.46)$$

where $\hat{J}_{\hat{n}}$ is the instantaneous cost function, \hat{J} is the global cost function, and \hat{n} is the discrete time steps. If the weights are updated at each time step in order to minimize the instantaneous cost function, this learning mode is called pattern learning, and if the weights are updated once for all time steps so that the global cost function \hat{J} is reduced, this learning mode is known as batch learning. An optimal control algorithm using NN based on the pattern learning mode is presented in [63]. The steepest-descent method is used here as the weight updating rule.

One multilayer NN controller with a single hidden layer is presented in [87]. The optimal number of hidden neurons is selected after performing a number of iterative training cycles. The network will generate an active control force as output using the structure response as its input. The batch learning is used here, where the network weights and biases are selected in such a way that a minimal objective cost function is achieved. The steepest-gradient-descent optimization method is used for the weight update, where the partial-differential equations are solved using the chain rule.

Probabilistic neural networks (PNN) are feed-forward networks built with three layers. They are derived from Bayes decision networks that estimates the probability density function for each class based on the training samples. The PNN trains immediately but execution time is slow and it requires a large amount of memory space. A new method to prepare the training pattern and to calculate PNN output (control force) quickly is proposed in [88]. The training patterns are uniformly distributed at the lattice point in state-space, so that the position of invoked input can be known. This type of network is called as Lattice probabilistic neural network (LPNN). The

calculation time is reduced by considering only the adjacent patterns. Here, the distance between the input pattern (response of structure) and training patterns (lattice type) for LPNN are calculated, which is then converted as the weights.

An active type NN controller using one counterpropagation network (CPN) is presented in [89], which is an unsupervised learning type NN, so that the control force is generated without any target control forces. Another intelligent control technique using a NN is proposed for seismic protection of offshore structures [65].

The ability of the nets to perform nonlinear mappings between the inputs and outputs, and to adapt its parameters so as to minimize an error criterion, make the use of ANN particularly well suited for the identification of both linear and nonlinear dynamic systems. The NN for system identification in structural control applications were presented in [40]. A NN is designed to approximate the nonlinear structural system and the corresponding stability conditions are derived [82]. A state-feedback controller for the NN is designed using a linear differential inclusion (LDI) state-space representation, which is useful in the stability analysis. Using NN, the system in (2.14) is approximated as a LDI representation with less modeling errors.

An intelligent structural control system with improved BP-NN is proposed in [90], which is used to predict the inverse model of the MR damper and for eliminating time-delay in the system. The system represented in (2.14) is considered here. The system has two controllers; the first one modifies the actual structural model, which was offline trained before and the second controller causes error emendation by means of online feedback. A multilayer NN for structural identification and prediction of the earthquake input is presented in [91].

Fuzzy Logic Control. Like NN, Fuzzy logic is also a model free approach for system identification and control. The FLC design involves; the selection of the input, output variables, and data manipulation method, membership function, and rule base design. Due to its simplicity, nonlinear mapping capability, and robustness, the FLC has been used in many structural control applications [92].

A FLC is designed [78] for a 15-story structure with two type of actuators, one mounted on the first floor and the other actuator (ATMD) on the fifteenth floor. The proposed FLC uses the position error and their derivatives as the input variable to produce the control forces for each actuator. The rule base is formed using seven fuzzy variables. The controller uses Mamdani method for fuzzification and Centroid method for defuzzification. A simulation using Kocaeli earthquake signal is carried out to prove the improvement in the performance of the FLC. A similar type of FLC is presented in [93], for the active control of wind excited tall buildings using ATMD. Another FLC for MDOF is proposed [94], that uses the same architecture, which is further modified into MDOF using weighted displacement and weighted velocity. In order to get the maximum displacement and velocity values, a high magnitude earthquake is used to excite the building structure. As all the floors do not have control devices, a weighting value is assigned to each floor, which will be large if the control device is closer to that particular floor. Finally, a force factor is calculated based on the weights of each floor.

A Fuzzy based on-off controller is designed to control the structural vibration using a semi-active TLCD [95]. The optimal control force is given as

$$u = - \sum_{i=1}^r p_i z_i \quad (2.47)$$

where $p_i = [p_1, \dots, p_r]$ is the optimal control gain vector obtained using LQR strategy. The control force will act opposite to the direction of the liquid velocity (\dot{x}_f). The regulation of the control force is done by varying the coefficient of headloss (ξ) with the semi-active control rule as given below.

$$\xi(t) = \begin{cases} \xi_{max} & \text{if } \{z_l(t)\dot{x}_f(t)\} < 0 \\ \xi_{min} & \text{if } \{z_l(t)\dot{x}_f(t)\} \geq 0 \end{cases} \quad (2.48)$$

where z_l represents the largest weighted state, which contributes most of the control force in (2.47). Finally, using the above control law a FLC is designed, that takes the liquid velocity and the large weighted displacement ($z_i = z_l$) as its input and produces the coefficient of headloss as the output, which is used to control the valve in the semi-active TLCD.

A fuzzy supervisory control method is presented in [96], which has a fuzzy supervisor in the higher level and three subcontrollers in the lower level. First, the subcontrollers are designed based on the LQR strategy, where the three subcontrollers are derived from three different weight matrices. The fuzzy-supervisor tunes these subcontrollers according to the structure's current behavior. A similar work is done in [56], where the subcontroller is designed using an optimal controller in the modal space. The matrix in the Riccati equation is calculated using the natural frequencies of the dominant modes and a corresponding gain matrix is determined. Another FLC for active control of structure using modal space is presented in [97], which uses a Kalman filter as an observer for the modal state estimation and a low-pass filter for eliminating the spillover problem.

Instead of using a mathematical model, a black-box based controller is proposed in [98]. Here, the force-velocity characteristics of the MR damper corresponding to different voltages are obtained experimentally, which are used to calculate the desired control force. The effect of the damper position and capacity on the control response is also studied.

An alternative to the conventional FLC, using an algebraic method is proposed in [99]. Here, the hedge algebra is used to model the linguistic domains and variables and their semantic structure is obtained. Instead of performing fuzzification and defuzzification, more simple methods are adopted, termed as semantization and desemantization, respectively. The hedge algebra-based fuzzy system is a new topic, which was first applied to fuzzy control in 2008. Compared to the classic FLC, this method is simple, effective, and can be easily interpreted.

Some structural vibration controllers were designed, where the FLC is combined with the GA [5]. The GA is known for its optimization capabilities. The GA is used here to optimize different parameters in the FLC like its rule base and membership function.

Genetic Algorithm. The GA is an iterative and stochastic process that proceeds by creating successive generation of offsprings from parents by performing the operations like selection, crossover, and mutation. The above operation is performed based on the fitness (termed as cost function in optimization problems) value assigned to each individual. After these operations, the parents are replaced by the offsprings, which is continued till an optimal solution for the problem is attained [100].

The structural control problem consists of different objectives to be optimized, which can be formulated using multi-objective optimization algorithms like GA. In [101], a preference-based optimum design using GA for an active control of structure is proposed, where the structure and control system is treated as a combined system. Here, the structural sizing variables, locations of actuators, and the elements of the feedback gain matrix are considered as the design variables and the cost of structural members, required control efforts, and dynamic responses due to earthquakes are considered as the objective functions to be minimized. For each objective criterion, preference functions are defined in terms of degrees of desirability and regions that represent the degrees of desirability. They are categorized as desirable, acceptable, undesirable, and unacceptable with ranges defined by $(\lambda_i \leq c_{i1})$, $(c_{i1} \leq \lambda_i \leq c_{i2})$, $(c_{i2} \leq \lambda_i \leq c_{i3})$, and $(c_{i3} \leq \lambda_i)$ respectively, where c_{i1} , c_{i2} , and c_{i3} are the range boundary values and λ_i is the i -th design objective. The preference-based optimization problem model is then given as

$$F_P(\lambda) = \frac{1}{l} \sum_{i=1}^l f_{P_i}[\lambda_i(d)] \quad (2.49)$$

with $\lambda_i(d) < c_{i3}$ and $d_{min} \leq d \leq d_{max}$, where F_P is the aggregate preference function, f_P is the power function, l is the number of design objectives, and d is the vector of design variables; d_{min} and d_{max} are the prescribed design constraints, respectively. Finally, the fitness function of n_g randomly created strings is defined as follows

$$F_{f_i} = [\max(F_{P_j}) + \min(F_{P_j})] - F_{P_i} \quad j = 1, \dots, n_g \quad (2.50)$$

where F_{f_i} is the fitness value of i th individual. A numerical simulation of an earthquake excited 10-story building is carried out and the proposed algorithm is able to achieve improved performance with less control effort.

An active control of structures under wind excitations using a multilevel optimal design based on GA is proposed [25]. The proposed multilevel genetic algorithm (MLGA) considers the number and position of the actuators and control algorithm as multiple optimization problems. This problem has the properties of nonlinearity, noncontinuous, and multimodal objective function. In [102], a GA is used to tune the mass, damping, and stiffness of the MRF absorber.

In [18], a feedback controller is designed, where the feedback gains are optimized using a GA. The controller also considers the time-delay in applying control forces to the devices. Two objective functions are: (1) to reduce the displacement and acceleration response of the i th floor, and (2) to reduce the story drift response as shown in (2.51) and (2.52) respectively.

$$\alpha_1 \sum_{\hat{n}=1}^r x_i[\hat{n}]^2 + \alpha_2 \sum_{\hat{n}=1}^r \ddot{x}_i[\hat{n}]^2 \quad (2.51)$$

$$\max \left\{ \sum_{\hat{n}=1}^r \frac{|d_1[\hat{n}]|}{x_{m0}}, \sum_{\hat{n}=1}^r \frac{|d_2[\hat{n}]|}{x_{m0}}, \dots, \sum_{\hat{n}=1}^r \frac{|d_m[\hat{n}]|}{x_{m0}} \right\} \quad (2.52)$$

where α_1 and α_2 are the weights of displacement and acceleration responses respectively, $d_i[\hat{n}]$ is the story drift from the i th to $(i-1)$ th floor at the time data point \hat{n} , and x_{m0} is the maximum displacement responses in all stories. The effectiveness of the proposed method is demonstrated using numerical simulation of a 3-story and 8-story structures excited by different seismic forces.

The disadvantage of the GA is that, it requires long computational time if the number of variables involved in the computation increases. A modified GA strategy is proposed in [41] to improve the computational time efficiency, which uses the search space reduction method (SSRM) using a Modified GA based on migration and artificial selection (MGAMAS) strategy. In order to improve the computational performance, the algorithm utilizes some novel ideas including nonlinear cyclic mutation, tagging, and reduced data input

Sliding Mode Control. SMC is one of the most popular robust control techniques. A switching control law is used to drive the system's state trajectory onto a prespecified surface in the state-space and to maintain the system's state trajectory on this surface for subsequent time, which results in a globally asymptotically stable system. In the case of structural vibration control, this surface corresponds to a desired system dynamics. The robustness of the SMC against the uncertainties and parameter variations makes them a better choice for structural control applications.

The nonlinear control force in SMC is given as

$$u = u_{eq} - \eta \operatorname{sgn}(\sigma(t)) \quad (2.53)$$

where the linear term u_{eq} is the equivalent control force, $\sigma = [\sigma_1, \dots, \sigma_n]$ are the n sliding variables, and η is the design parameter that guarantees the system trajectories reach the sliding surface in finite time. A SMC with hybrid control is proposed in [103], where the control law also termed as reaching law is formed using the constant plus proportional rate reaching law and power rate reaching law.

Due to the imperfection in the high-frequency discontinuous switching, the direct implementation of the control given in (2.53) will result in chattering effect, which may cause damage to the mechanical components, hence the actuators. This effect should be eliminated by suitably smoothing the control force or by using continuous SMC. Many structural control strategies based on the non-chattering SMC were reported [79].

A modal space sliding mode control (MS-SMC) method is designed in [44], where the dominant frequencies are derived using power spectrum as well as the wavelet analysis of the time series of the input-output. SMC based on a single-mode (first

mode) reduced-order model is designed. Another SMC based on the modal analysis is presented in [104], where the first six modes of the structure were considered.

During seismic events, the main control unit may lose its functionality, so it is a better option to use a decentralized system, where the whole control is divided into subsystems and are controlled independently. Such a type of decentralized system with SMC is presented in [105]. The numerical studies were carried out for full control and partial control cases and reaching laws were derived for cases; with and without considering actuator saturations. They found that the full control case is more effective, and they could not find any significant changes in the control for different subsystem configurations.

A NN-based SMC for the active control of seismicity excited building structures is proposed in [106]. Here apart from the sliding variables, the matrix σ also represents the slope of the sliding surface. This slope moves in a stable region, which results in a moving sliding surface. A four layer feedforward NN is used to reduce chattering effect and to determine the sliding surface slope. To achieve a minimum performance index, the controller is optimized using a GA during the training process. It is shown that a high performing controller is achieved by using the moving sliding surface. Another SMC based on radial basis function (RBF) NN is reported in [107]. The chattering free SMC is obtained using a two-layered RBF-NN. The relative displacement of each floor is fed as the input to the NN and the design parameter η is taken as the output. A modified gradient-descent method is used for updating the weights.

Couple of research works were carried out in designing the SMC using Fuzzy logic so-called, fuzzy sliding mode control (FSMC) [108]. The SMC provides a stable and fast system, whereas the FLC provides the ability to handle a nonlinear system. The Chattering problem is avoided in most of these FSMC systems. A FSMC based on GA is presented in [109], where the GA is used to find the optimal rules and membership functions for the FLC.

References

1. J.T.P. Yao, Concept of structural control. *J. Struct. Div.* **98**, 1567–1574 (1972)
2. G.W. Housner, L.A. Bergman, T.K. Caughey, A.G. Chassiakos, R.O. Claus, S.F. Masri, R.E. Skelton, T.T. Soong, B.F. Spencer, J.T.P. Yao, Structural control: past, present and future. *J. Eng. Mech.* **123**, 897–974 (1997)
3. T. Balendra, C.M. Wang, N. Yan, Control of wind-excited towers by active tuned liquid column damper. *Eng. Struct.* **23**, 1054–1067 (2001)
4. S.L. Djajakesukma, B. Samali, H. Nguyen, Study of a semi-active stiffness damper under various earthquake inputs. *Earthq. Eng. Struct. Dyn.* **31**, 1757–1776 (2002)
5. G. Yan, L.L. Zhou, Integrated fuzzy logic and genetic algorithms for multi-objective control of structures using MR dampers. *J. Sound Vib.* **296**, 368–382 (2006)
6. F. Yi, S.J. Dyke, Structural control systems: performance assessment. *Proc. Am. Control Conf.* **1**, 14–18 (2000)
7. F.Y. Cheng, H. Jiang, K. Lou, *Smart Structures: Innovative Systems for Seismic Response Control* (CRC Press, Boca Raton, 2008)
8. Z. Liang, G.C. Lee, G.F. Dargush, J. Song, *Structural Damping: Applications in Seismic Response Modification* (CRC Press, Boca Raton, 2011)

9. N.R. Fisco, H. Adeli, Smart structures: part I—active and semi-active control. *Sci. Iran.* **18**, 275–284 (2011)
10. N.R. Fisco, H. Adeli, Smart structures: part II—hybrid control systems and control strategies. *Sci. Iran.* **18**, 285–295 (2011)
11. T.K. Datta, A state-of-the-art review on active control of structures. *ISSET J. Earthq. Technol.* **40**, 1–17 (2003)
12. S. Korkmaz, A review of active structural control: challenges for engineering informatics. *Comput. Struct.* **89**, 2113–2132 (2011)
13. A.C. Nerves, R. Krishnan, Active control strategies for tall civil structures. *Proc. IEEE Int. Conf. Ind. Electron. Control Instrum.* **2**, 962–967 (1995)
14. T.T. Soong, S.F. Masri, G.W. Housner, An overview of active structural control under seismic loads. *Earthq. Spectra* **7**, 483–505 (1991)
15. J.N. Yang, T.T. Soong, Recent advances in active control of civil engineering structures. *Probab. Eng. Mech.* **3**, 179–188 (1988)
16. B.F. Spencer, S. Nagarajaiah, State of the Art of structural control. *J. Struct. Eng.* **129**, 845–856 (2003)
17. T.T. Soong, B.F. Spencer, Supplemental energy dissipation: state-of-the-art and state-of-the-practice. *Eng. Struct.* **24**, 243–259 (2002)
18. B.F. Spencer, M.K. Sain, Controlling buildings: a new frontier in feedback. *IEEE Control Syst. Mag. Emerg. Technol.* **17**, 19–35 (1997)
19. M.D. Symans, M.C. Constantinou, Semi-active control systems for seismic protection of structures: a state-of-the-art review. *Eng. Struct.* **21**, 469–487 (1999)
20. G. Kerschen, K. Worden, A.F. Vakakis, J.C. Golinva, Past, present and future of nonlinear system identification in structural dynamics. *Mech. Syst. Signal Process.* **20**, 505–592 (2006)
21. S.B. Kim, C.B. Yun, Sliding mode fuzzy control: theory and verification on a benchmark structure. *Earthq. Eng. Struct. Dyn.* **29**, 1587–1608 (2000)
22. Y. Tang, Active control of SDF systems using artificial neural networks. *Comput. Struct.* **60**, 695–703 (1996)
23. S. Thenozhi, W. Yu, Advances in modeling and vibration control of building structures. *Annu. Rev. Control* **37**(2), 346–364 (2013)
24. B. Jiang, X. Wei, Y. Guo, Linear quadratic optimal control in active control of structural vibration systems, in *Control and Decision Conference, 2010 Chinese*, vol 98, pp. 3546–3551 (2010)
25. Q.S. Li, D.K. Liu, J.Q. Fang, C.M. Tam, Multi-level optimal design of buildings with active control under winds using genetic algorithms. *J. Wind Eng. Ind. Aerodyn.* **86**, 65–86 (2000)
26. A.K. Chopra, *Dynamics of Structures: Theory and application to Earthquake engineering*, 2nd edn. (Prentice Hall, 2001)
27. Y.K. Wen, Method for random vibration of hysteretic systems. *J. Eng. Mech.* **102**, 249–263 (1976)
28. F. Ikhouane, V. Mañosa, J. Rodellar, Dynamic properties of the hysteretic Bouc-Wen model. *Syst. Control Lett.* **56**, 197–205 (2007)
29. F. Amini, M.R. Tavassoli, Optimal structural active control force, number and placement of controllers. *Eng. Struct.* **27**, 1306–1316 (2005)
30. M. Guney, E. Eskinat, Optimal actuator and sensor placement in flexible structures using closed-loop criteria. *J. Sound Vib.* **312**, 210–233 (2008)
31. W. Gawronski, Actuator and Sensor placement for structural testing and control. *J. Sound Vib.* **208**, 101–109 (1997)
32. W. Liu, Z. Hou, M.A. Demetriou, A computational scheme for the optimal sensor/actuator placement of flexible structures using spatial H_2 measures. *Mech. Syst. Sig. Process.* **20**, 881–895 (2006)
33. D.K. Liu, Y.L. Yang, Q.S. Li, Optimum positioning of actuators in tall buildings using genetic algorithm. *Comput. Struct.* **81**, 2823–2827 (2003)
34. L. Ljung, *System Identification Theory for the Users* (Prentice-Hall Inc, New Jersey, 1987)

35. H. Imai, C.B. Yun, O. Maruyama, M. Shinozuka, Fundamentals of system identification in structural dynamics. *Probab. Eng. Mech.* **4**, 162–173 (1989)
36. J. Zhang, P.N. Roschke, Active control of a tall structure excited by wind. *J. Wind Eng. Ind. Aerodyn.* **83**, 209–223 (1999)
37. D.P. Mandic, J.A. Chambers, *Recurrent Neural Networks for Prediction: Learning Algorithms, Architectures and Stability* (Wiley, Hoboken, 2001)
38. S.L. Hung, C.S. Huang, C.M. Wen, Y.C. Hsu, Nonparametric identification of a building structure from experimental data using wavelet neural network. *Comput. Aided Civ. Infrastruct. Eng.* **18**, 356–368 (2003)
39. F. Plestana, Y. Shtessel, V. Bregeault, A. Poznyak, New methodologies for adaptive sliding mode control. *Int. J. Control* **83**, 1907–1919 (2010)
40. B. Xu, Z. Wu, G. Chen, K. Yokoyama, Direct identification of structural parameters from dynamic responses with neural networks. *Eng. Appl. Artif. Intell.* **17**, 931–943 (2004)
41. M.J. Perry, C.G. Koh, Y.S. Choo, Modified genetic algorithm strategy for structural identification. *Comput. Struct.* **84**, 529–540 (2006)
42. W.H. Zhu, Velocity estimation by using position and acceleration sensors. *IEEE Trans. Ind. Electron.* **54**, 2706–2715 (2007)
43. D.M. Boore, Analog-to-Digital conversion as a source of drifts in displacements derived from digital recordings of ground acceleration. *Bull. Seismol. Soc. Am.* **93**, 2017–2024 (2003)
44. R. Adhikari, H. Yamaguchi, T. Yamazaki, Modal space sliding-mode control of structures. *Earthq. Eng. Struct. Dyn.* **27**, 1303–1314 (1998)
45. C.M. Casado, I.M. Díaz, J.D. Sebastián, A.V. Poncela, A. Lorenzana, Implementation of passive and active vibration control on an in-service footbridge. *Struct. Control Health Monit.* **20**, 70–87 (2013)
46. F.L. Lewis, D.M. Dawson, C.T. Abdallah, *Robot Manipulator Control: Theory and Practice*, 2nd edn. (Marcel Dekker, Inc, 2004)
47. S.F. Ali, A. Ramaswamy, Optimal fuzzy logic control for MDOF structural systems using evolutionary algorithms. *Eng. Appl. Artif. Intell.* **22**, 407–419 (2009)
48. K.J. Åström, T. Hägglund, Revisiting the Ziegler-Nichols step response method for PID control. *J. Process Control* **14**, 635–650 (2004)
49. Z.Q. Gu, S.O. Oyadiji, Application of MR damper in structural control using ANFIS method. *Comput. Struct.* **86**, 427–436 (2008)
50. Y.K. Thong, M.S. Woolfson, J.A. Crowe, B.R.H. Gill, D.A. Jones, Numerical double integration of acceleration measurements in noise. *Measurement* **36**, 73–92 (2004)
51. T.S. Edwards, Effects of aliasing on numerical integration. *Mech. Syst. Sign. Process.* **21**, 165–176 (2007)
52. K. Worden, Data processing and experiment design for the restoring force surface method, part I: integration and differentiation of measured time data. *Mech. Syst. Sign. Process.* **4**, 295–319 (1990)
53. H.P. Gavin, R. Morales, K. Reilly, Drift-free integrators. *Rev. Sci. Instrum.* **69**, 2171–2175 (1998)
54. J.G.T. Ribeiro, J.T.P. de Castro, J.L.F. Freire, Using the FFT-DDI method to measure displacements with piezoelectric, resistive and ICP accelerometers. *Conf. Expo. Struct. Dyn.* (2003)
55. J. Yang, J.B. Li, G. Lin, A simple approach to integration of acceleration data for dynamic soil-structure interaction analysis. *Soil Dyn. Earthq. Eng.* **26**, 725–734 (2006)
56. K.S. Park, H.M. Koh, C.W. Seo, Independent modal space fuzzy control of earthquake-excited structures. *Eng. Struct.* **26**, 279–289 (2004)
57. S.H. Razavi, A. Abolmaali, M. Ghassemieh, A weighted residual parabolic acceleration time integration method for problems in structural dynamics. *J. Comput. Methods Appl. Math.* **7**, 227–238 (2007)
58. R. Kelly, A tuning procedure for stable PID control of robot manipulators. *Robotica* **13**, 141–148 (1995)

59. C.M. Chang, B.F. Spencer, Active base isolation of buildings subjected to seismic excitations. *Earthq. Eng. Struct. Dyn.* **39**, 1493–1512 (2010)
60. M.D. Iuliis, C. Faella, Effectiveness analysis of a semiactive base isolation strategy using information from an early-warning network. *Eng. Struct.* **52**, 518–535 (2013)
61. K.C.S. Kwok, B. Samali, Performance of tuned mass dampers under wind loads. *Eng. Struct.* **17**, 655–667 (1995)
62. R. Saragih, Designing Active vibration control with minimum order for flexible structures. *IEEE Int. Conf. Control Autom.* 450–453 (2010)
63. J.T. Kim, H.J. Jung, I.W. Lee, Optimal structural control using neural networks. *J. Eng. Mech.* **126**, 201–205 (2000)
64. G. Miwada, O. Yoshida, R. Ishikawa, M. Nakamura, Observation records of base-isolated buildings in strong motion area during the 2011 off the Pacific Coast of Tohoku earthquake, in *Proceedings of the International Symposium on Engineering Lessons Learned from the 2011 Great East Japan Earthquake* (2012), pp. 1017–1024
65. D.H. Kim, Neuro-control of fixed offshore structures under earthquake. *Eng. Struct.* **31**, 517–522 (2009)
66. T.T. Soong, *Active Structural Control: Theory and Practice* (Longman, New York, 1990)
67. T.T. Soong, A.M. Reinhorn, Y.P. Wang, R.C. Lin, Full-scale implementation of active control-I: design and simulation. *J. Struct. Eng.* **117**, 3516–3536 (1991)
68. J.C.H. Chang, T.T. Soong, Structural control using active tuned mass damper. *J. Eng. Mech. ASCE* **106**, 1091–1098 (1980)
69. A. Alavinasab, H. Moharrami, Active control of structures using energy-based LQR method. *Comput. Aided Civ. Infrastruct. Eng.* **21**, 605–611 (2006)
70. A. Forrai, S. Hashimoto, H. Funato, K. Kamiyama, Structural control technology: system identification and control of flexible structures. *Comput. Control Eng. J.* **402**, 1–40 (2001)
71. D. Hrovat, P. Barak, M. Rabins, Semi-active versus passive or active tuned mass dampers for structural control. *J. Eng. Mech.* **109**, 691–705 (1983)
72. Z. Xu, A.K. Agrawal, J.N. Yang, Semi-active and passive control of the phase I linear base-isolated benchmark building model. *Struct. Control Health Monit.* **13**, 626–648 (2006)
73. J. Pandya, Z. Akbay, M. Uras, H. Aktan, *Exp. Implement. Hybrid Control* (Proceedings of Structures Congress XIV, Chicago, 1996)
74. B.F. Spencer, S.J. Dyke, M.K. Sain, J.D. Carlson, Phenomenological model of a magnetorheological damper. *J. Eng. Mech. ASCE* **123**, 230–238 (1997)
75. Y.L. Xu, B. Chen, Integrated vibration control and health monitoring of building structures using semi-active friction dampers: Part I-methodology. *Eng. Struct.* **30**, 1789–1801 (2008)
76. W. Park, K.S. Park, H.M. Koh, Active control of large structures using a bilinear pole-shifting transform with H_∞ control method. *Eng. Struct.* **30**, 3336–3344 (2008)
77. O.I. Obe, Optimal actuators placements for the active control of flexible structures. *J. Math. Anal. Appl.* **105**, 12–25 (1985)
78. R. Guclu, H. Yazici, Vibration control of a structure with ATMD against earthquake using fuzzy logic controllers. *J. Sound Vib.* **318**, 36–49 (2008)
79. R. Guclu, Sliding mode and PID control of a structural system against earthquake. *Math. Comput. Model.* **44**, 210–217 (2006)
80. T.L. Teng, C.P. Peng, C. Chuang, A study on the application of fuzzy theory to structural active control. *Comput. Methods Appl. Mech. Eng.* **189**, 439–448 (2000)
81. V.I. Utkin, *Sliding Modes in Control and Optimization* (Springer, Berlin, 1990)
82. C.W. Chen, Modeling and control for nonlinear structural systems via a NN-based approach. *Expert Syst. Appl.* **36**, 4765–4772 (2009)
83. H. Du, N. Zhang, H_∞ control for buildings with time delay in control via linear matrix inequalities and genetic algorithms. *Eng. Struct.* **30**, 81–92 (2008)
84. K. Seto, A structural control method of the vibration of flexible buildings in response to large earthquake and strong winds, in *Proceedings of the 35th Conference on Decision and Control* (Kobe, Japan, 1996)

85. S. Pourzeynali, H.H. Lavasani, A.H. Modarayi, Active control of high rise building structures using fuzzy logic and genetic algorithms. *Eng. Struct.* **29**, 346–357 (2007)
86. Y.K. Wen, J. Ghaboussi, P. Venini, K. Nikzad, Control of structures using neural networks. *Smart Mater. Struct.* **4**, 149–157 (1995)
87. H.C. Cho, M.S. Fadali, M.S. Saiedi, K.S. Lee, Neural network active control of structures with earthquake excitation. *Int. J. Control Autom. Syst.* **2**, 202–210 (2005)
88. D.H. Kim, D. Kimb, S. Chang, H.Y. Jung, Active control strategy of structures based on lattice type probabilistic neural network. *Probab. Eng. Mech.* **23**, 45–50 (2008)
89. A. Madan, Vibration control of building structures using self-organizing and self-learning neural networks. *J. Sound Vib.* **287**, 759–784 (2005)
90. J. Liu, K. Xia, C. Zhu, Structural vibration intelligent control based on magnetorheological damper, in *International Conference on Computational Intelligence and Software Engineering* (2009), pp. 1–4
91. A. Tani, H. Kawamura, S. Ryu, Intelligent fuzzy optimal control of building structures. *Eng. Struct.* **20**, 184–192 (1998)
92. E. Reithmeier, G. Leitmann, Structural vibration control. *J. Franklin Inst.* **338**, 203–223 (2001)
93. M. Aldawod, F. Naghdy, B. Samali, K.C.S. Kwok, Active control of wind excited structures using fuzzy logic, in *IEEE International Fuzzy Systems Conference Proceedings* (1999), pp. 72–77
94. K. Yeh, W.L. Chiang, D.S. Juang, Application of fuzzy control theory in active control of structures, in *IEEE Proceeding NAFIPS/IFIS/NASA* (1994), pp. 243–247
95. S.K. Yalla, A. Kareem, J.C. Kantor, Semi-active tuned liquid column dampers for vibration control of structures. *Eng. Struct.* **23**, 1469–1479 (2001)
96. K.S. Park, H.M. Koh, S.Y. Ok, Active control of earthquake excited structures using fuzzy supervisory technique. *Adv. Eng. Softw.* **33**, 761–768 (2002)
97. K.M. Choi, S.W. Cho, D.O. Kim, I.W. Lee, Active control for seismic response reduction using modal-fuzzy approach. *Int. J. Solids Struct.* **42**, 4779–4794 (2005)
98. D. Das, T.K. Datta, A. Madan, Semiactive fuzzy control of the seismic response of building frames with MR dampers. *Earthq. Eng. Struct. Dyn.* **41**, 99–118 (2012)
99. N.D. Duc, N.L. Vu, D.T. Tran, H.L. Bui, A study on the application of hedge algebras to active fuzzy control of a seism-excited structure. *J. Vib. Control*, 1–15 (2011)
100. P.J. Fleming, R.C. Purshouse, Evolutionary algorithms in control systems engineering: a survey. *Control Eng. Pract.* **10**, 1223–1241 (2002)
101. K.S. Park, H.M. Koh, Preference-based optimum design of an integrated structural control system using genetic algorithms. *Adv. Eng. Softw.* **35**, 85–94 (2004)
102. L.J. Li, MRF absorber damping control for building structural vibration response by means of genetic optimum algorithm. *Adv. Mater. Res.* **219–220**, 1133–1137 (2011)
103. B. Zhao, X. Lu, M. Wu, Z. Mei, Sliding mode control of buildings with base-isolation hybrid protective system. *Earthq. Eng. Struct. Dyn.* **29**, 315–326 (2000)
104. M. Allen, F.B. Zazzera, R. Scattolini, Sliding mode control of a large flexible space structure. *Control Eng. Pract.* **8**, 861–871 (2000)
105. S.M. Nezhad, F.R. Rofooei, Decentralized sliding mode control of multistory buildings. *Struct. Des. Tall Spec. Build.* **16**, 181–204 (2007)
106. O. Yakut, H. Alli, Neural based sliding-mode control with moving sliding surface for the seismic isolation of structures. *J. Vib. Control* **17**, 2103–2116 (2011)
107. Z. Li, Z. Deng, Z. Gu, New sliding mode control of building structure using RBF neural networks. *Chin. Control Decis. Conf.* 2820–2825 (2010)
108. H. Alli, O. Yakut, Fuzzy sliding-mode control of structures. *Eng. Struct.* **27**, 277–284 (2005)
109. A.P. Wang, Y.H. Lin, Vibration control of a tall building subjected to earthquake excitation. *J. Sound Vib.* **299**, 757–773 (2007)

Active Structural Control with Stable Fuzzy PID
Techniques

Yu, W.; Thenozhi, S.

2016, VI, 124 p. 88 illus., 18 illus. in color., Softcover

ISBN: 978-3-319-28024-0